

Molecular imaging of bone metastases and their response to therapy.

Gary J. R. Cook (ORCID: 0000-0002-8732-8134)

Vicky Goh (ORCID: 0000-0002-2321-8091)

Cancer Imaging Department, School of Biomedical Engineering and Imaging Sciences, Kings College
London, UK.

Correspondence to:

Professor Gary Cook, Clinical PET Centre, St Thomas' Hospital, London. SE1 7EH. UK.

Tel: ++44 (0)207 188 8364 Fax: ++44 (0)207 620 0790 Email: gary.cook@kcl.ac.uk

Running title: Imaging bone metastases

ACKNOWLEDGEMENTS

The authors acknowledge financial support from the Department of Health via the National Institute for Health Research (NIHR) Biomedical Research Centre awards to Guy's & St Thomas' NHS Foundation Trust in partnership with King's College London and the King's College London / University College London Comprehensive Cancer Imaging Centres funded by Cancer Research UK and Engineering and Physical Sciences Research Council in association with the Medical Research Council and the Department of Health (England) and a research grant from Breast Cancer now.

Figure 4 courtesy of Blue Earth Diagnostics Ltd.

DISCLOSURE STATEMENT

GC was a co-investigator in the FALCON trial (NCT02578940).

No other potential conflicts of interest relevant to this article exist.

RUNNING TITLE

Molecular imaging of bone metastases

ABSTRACT

Bone metastases are common, especially in more prevalent malignancies such as breast and prostate cancer. They cause significant morbidity and draw on healthcare resources.

Molecular and hybrid imaging techniques, including single photon emission computed tomography with computed tomography (SPECT/CT), positron emission tomography / CT and whole-body MRI with diffusion-weighted imaging (WB-MRI), have improved diagnostic accuracy in staging the skeleton compared to previous standard imaging methods, allowing earlier tailored treatment.

With the introduction of several effective treatment options, it is now even more important to detect and monitor response in bone metastases accurately. Conventional imaging, including radiographs, CT, MRI and bone scintigraphy, are recognized as being insensitive and non-specific for response monitoring in a clinically relevant time frame. Early reports of molecular and hybrid imaging techniques, as well as WB-MRI, promise earlier and more accurate prediction of response vs non-response but have yet to be adopted routinely in clinical practice.

We summarize the role of new molecular and hybrid imaging methods including SPECT/CT, PET/CT and WB-MRI. These modalities are associated with improvements in diagnostic accuracy for staging and response assessment of skeletal metastases over standard imaging methods, being able to quantify biological processes related to the bone microenvironment as well as tumor cells. The described improvements in the imaging of bone metastases and their response to therapy have led to some being adopted into routine clinical practice in some centers and at the same time provide better methods to assess treatment response of bone metastases in clinical trials.

KEY WORDS

Bone metastases; bone scintigraphy; SPECT/CT; PET/CT; whole-body MRI

INTRODUCTION

Bone metastases from most cancers are associated with an increased risk of skeletal-related events (SREs), including pathological fracture, spinal cord compression and may need radiotherapy or surgery for pain or impending fracture. Morbidity may also be associated with bone marrow suppression and hypercalcemia. Bone metastases are common in two of the most prevalent cancers, i.e. breast and prostate cancer, where up to 65-90% and 65-75% of patients, respectively with advanced disease may be affected (1). There is some evidence that patients with bone-predominant metastatic disease have better survival than those with visceral disease and that oligometastatic disease has a more favorable prognosis, implying that early diagnosis may impact outcomes. The introduction of molecular and hybrid imaging techniques has improved sensitivity for bone metastases detection but there remains uncertainty as to which modality is optimal in each type of cancer.

With the introduction of several novel therapeutics for metastatic prostate and breast cancer, and a requirement for more personalized and nuanced decisions on the correct management strategy, it has become even more important that bone metastases are detected earlier so that therapy that reduces SREs can be instigated. In particular, the trend for treating oligometastatic disease with curative intent relies on sensitive diagnostics (2). Despite improved systemic therapeutics, response rates remain generally less than 50%. Therefore, it is important that non-responding patients are identified as soon as possible allowing transition to second-line therapy, to avoid potential toxicity from ineffective treatment and to optimally manage health care costs (3,4). This is especially important in metastatic breast and prostate cancers where survival tends to be longer than in patients with bone metastases from other cancers, with a subsequent greater impact on long-term morbidity and health care costs.

Imaging, and in particular molecular and hybrid imaging, has an increasing role in detecting bone metastases early in their evolution and in monitoring treatment response at early time points (Table 1) (5,6).

Bone scintigraphy, using ^{99m}Tc -labeled diphosphonates such as ^{99m}Tc -methylene diphosphonate (^{99m}Tc -MDP), has been used since the 1970s for detecting skeletal metastases and monitoring therapy, but it is recognized that sensitivity and specificity are limited at staging and for monitoring treatment response. Conventional imaging, e.g. radiographs, computed tomography (CT) or magnetic resonance imaging (MRI), that relies on size-based criteria for assessing treatment response, e.g. Response Evaluation Criteria in Solid Tumors (RECIST) (7), is also limited as bone disease is usually considered non-measurable unless associated with a measurable soft tissue component. Attempts have been made to incorporate bone scintigraphy with other imaging in breast cancer (8) and prostate cancer (9) to improve response assessment but early assessment within a clinically relevant time frame remains problematic in clinical practice. For example, the Prostate Cancer Working Group criteria primarily aim to determine disease progression, requiring at least 2 new lesions on the first assessment following a baseline bone scan and then at least a further 2 lesions on a subsequent confirmatory scan before progressive disease is confirmed (9). Scans are recommended every 8 to 9 weeks for the first 24 weeks and every 12 weeks thereafter.

The combination of either tumor or bone-specific radiotracers with CT or MRI in hybrid scanners, e.g. single photon emission computed tomography (SPECT/CT), positron emission tomography /CT (PET/CT) or PET/MRI, has potential to improve diagnosis and response assessment with synergy between morphological and molecular information. However, despite the potential for gathering multiparametric information from metastases that reports on diverse underlying biological and morphological tumor characteristics, there have been relatively few reports that have successfully exploited these potential benefits.

The purpose of this educational review is to update on the current status of functional and hybrid imaging, particularly PET and functional MRI methods, in detection and therapy response monitoring of bone metastases.

PATHOPHYSIOLOGY OF BONE METASTASES RELEVANT TO IMAGING

Paget's 'seed and soil' hypothesis, that metastatic cancer cells preferentially deposit in the marrow microenvironment in which they grow and eventually cause bone destruction, is relevant to skeletal metastasis imaging (10) as there is an opportunity to detect early marrow-based disease before a reaction in the bone microenvironment has occurred. This requires bone marrow or tumor-specific imaging methods, e.g. whole-body MRI (WB-MRI) with diffusion-weighted imaging or ^{18}F -Fluorodeoxyglucose (^{18}F -FDG) PET, for detection. These have therefore shown greater sensitivity than methods that require increased osteoblastic activity (e.g. X-rays, CT, bone scintigraphy, ^{18}F -Fluoride PET) which is a later event.

Biologic and morphologic characteristics of treatment-naïve bone metastases vary on a spectrum from predominantly lytic to predominantly sclerotic in nature, although both processes are usually present to some extent. Osteolytic metastases are commoner in most cancers (e.g. breast, lung). Here, cancer cells produce parathyroid hormone-related protein inducing osteoblasts to produce receptor activator of nuclear factor- κB ligand (RANKL) which stimulates osteoclast maturation and activity (11). Increased osteoclast activity leads to localized resorption of bone that exceeds the ability of osteoblasts to repair and releases factors from the bone matrix that stimulate parathyroid hormone-related protein production, thereby creating a vicious cycle. The resultant lytic lesions lead to the morbidity associated with bone metastases and SREs.

In some cancers, an osteoblastic phenotype predominates, e.g. prostate cancer. Tumor-derived growth factors primarily stimulate osteoblasts rather than osteoclasts. Excess abnormal bone is laid down with resultant sclerosis on radiographs and CT and increased activity on bone-specific nuclear medicine methods such as bone scintigraphy with $^{99\text{m}}\text{Tc}$ -MDP or ^{18}F -fluoride PET. Osteoblast activity may also increase as a reparative process in successfully treated bone metastases such that both lytic and sclerotic lesions become denser on radiographs or CT (12). This phenomenon

can also lead to an increase in uptake of bone-specific tracers such as ^{99m}Tc -MDP or ^{18}F -Fluoride. The so-called 'flare phenomenon', that causes an increase in activity in pre-existing metastases for several weeks or months, or the appearance of previously occult metastases after successful systemic therapy, has been well described and if seen is associated with an improved prognosis (13,14). This is due to an increase in reparative osteoblastic activity as the bone surrounding metastatic tumor cells heals following tumoricidal therapy.

Bone metastasis imaging can be divided into bone-specific or tumor-specific modalities, whether morphologic or functional. Morphologic methods that rely mostly on changes to bone density include radiographs or CT, although tumor-related soft tissue can also sometimes be appreciated on CT. Bone-specific nuclear medicine methods include bone scintigraphy (e.g. ^{99m}Tc -MDP) +/- SPECT or SPECT/CT) and ^{18}F -Fluoride PET/CT. Accumulation of these tracers reflects local blood flow and mineralization due to osteoblast activity (15). Although these agents predominantly rely on an osteoblastic mechanism for uptake and are therefore most sensitive in cancers associated with an osteoblastic phenotype (e.g. prostate cancer), most cancers associated with an osteolytic metastatic phenotype also show accumulation as there is usually an accompanying osteoblastic component (11). Some skeletal malignancies, such as myeloma, are predominantly osteolytic with suppressed bone formation and bone scintigraphy or ^{18}F -Fluoride PET may be relatively insensitive compared to tumor-specific methods.

Tumor-specific imaging methods that take advantage of different biological characteristics in tumor cells to provide contrast in the image, include MRI as well as PET and SPECT methods that use metabolic or receptor-targeting tracers.

Conventional MRI sequences (e.g. T1-weighted, T2-weighted, short tau inversion recovery), reflecting differences in proton density (i.e. water), detect tumor tissue within bone marrow and any soft tissue component invading bone. Diffusion-weighted MRI (DW-MRI) signal depends on restricted motion of water molecules and can be quantified by measuring the apparent diffusion coefficient (ADC),

allowing serial measurements to monitor treatment response (16). Tumors that are usually more highly cellular than normal tissues or normal bone marrow show greater restriction of water molecule motion. During successful treatment, water molecule motion is less restricted as tumors become less cellular and this effect can be seen with an increase in ADC. It is now possible to perform WB-MRI with conventional sequences and diffusion-weighted imaging in less than 1 hour and this method is now more frequently used to detect and monitor skeletal metastases. More recently, ultrashort echo time (UTE) MRI sequences have also shown promise in depicting the bone microstructure in humans and changes in mineralization to therapy in animal models (17).

Molecular imaging methods that are used for evaluating bone metastases include metabolic tracers, most commonly ^{18}F -FDG (5,6,18). Uptake of ^{18}F -FDG is enhanced in most malignant tumor cells by the Warburg effect resulting in increased glycolysis rather than oxidative metabolism (19). An increase in glucose membrane transporters and phosphorylation by hexokinase II leads to increased ^{18}F -FDG tumor accumulation compared to normal cells. Alternative metabolic tracers such as $^{18}\text{F}/^{11}\text{C}$ -Choline (choline kinase activity and cell membrane turnover) may be used in tumors such as prostate cancer that do not tend to show increased glycolysis (16).

Another metabolic PET tracer that has been licensed for biochemical recurrence of prostate cancer is ^{18}F -Fluciclovine. This synthetic amino acid analog of leucine shows increased uptake in tumor cells, reflecting increased amino acid transport, protein and nucleotide synthesis. There are preclinical and clinical reports of successful imaging of bone metastases with ^{18}F -Fluciclovine (20,21) despite normal diffuse bone marrow uptake. Other tracers that have shown efficacy in skeletal and soft tissue metastases include those targeting specific receptors or antigens. Small molecule inhibitors of prostate-specific membrane antigen (PSMA) labeled with ^{68}Ga show little normal bone marrow activity and are associated with good tumor to background contrast in bone metastases (22).

BONE-SPECIFIC IMAGING

Bone Scintigraphy Including SPECT and SPECT/CT

Bone scintigraphy with ^{99m}Tc -radiolabeled diphosphonates started in the 1970s. These tracers showed rapid clearance from blood and soft tissues with resultant good image contrast as early as 2 hours post injection (23). Although widely used for many decades for detecting and monitoring skeletal metastases, it is recognized that alternative modern imaging techniques are more sensitive and specific (5,6,16,18). However, the advent of SPECT image acquisition, and then hybrid imaging with SPECT/CT, has prolonged the life of bone scintigraphy. These hardware and reconstruction modifications improve both sensitivity (better contrast resolution) and specificity (3-dimensional display of data with CT anatomical correlate) (24,25). Combining CT morphological characteristics improves specificity of bone scintigraphy, with more accurate characterization of benign and malignant “hot spots” with an increase in confidence in scan interpretation and fewer equivocal studies (25) (Fig. 1).

Bone scintigraphy is recognized as being relatively insensitive and non-specific in the evaluation of systemic treatment response in skeletal metastases, often requiring several weeks or months before response can be confirmed (26). The flare phenomenon can make it impossible to differentiate progressive disease from a healing osteoblastic response for several weeks or months following chemotherapy or endocrine therapy. However, if a flare is recognized then it is a good prognostic sign (13).

^{18}F -Fluoride PET/CT

^{18}F -Fluoride was first described as a bone-specific tracer in 1962 but the high energy 511 keV photons are unsuited to gamma camera imaging and so it was not used clinically to much extent until the advent of modern PET and PET/CT scanners. Periodic shortages of ^{99m}Tc generators has also led to an increase in its use for functional bone imaging.

Regional accumulation of the tracer in the skeleton depends on local blood flow and mineralization activity with fluoride ions replacing hydroxyl ions in hydroxyapatite crystals to form fluoroapatite in bone mineral. With rapid clearance of soft tissue background activity by renal excretion, and near 100% first pass extraction by bone, good skeleton to background contrast can be achieved as early as 1-hour post injection (15) (Fig. 2a).

PET has the advantage of accurate and absolute quantification of tracer concentration, and although not generally suited to the clinic, it is possible to measure lesion blood flow (K_1 , ^{18}F -Fluoride clearance from plasma to bone tissue) and mineralization activity (K_i , plasma clearance to the bone mineral compartment) (15). These kinetic indices require dynamic scan acquisitions and direct or indirect measurement of the arterial plasma concentration of ^{18}F -Fluoride over time. Dynamic scans are generally limited to the length of the Z-axis of the PET scanner field of view and therefore not suited for whole body bone metastasis assessment. However, the kinetic method has been shown to be feasible as an adjunct to whole-body imaging in breast cancer related bone metastases (27) and as a method to measure response to dasatinib in prostate cancer bone metastases (28). To overcome the limited field of view for dynamic studies, a static whole skeleton scan method has been developed that measures K_i with the requirement for only two venous blood samples. This method was better at differentiating responders from non-responders in a small cohort of breast cancer patients with bone-predominant metastatic disease compared to standardized uptake values (29).

The superior contrast and spatial resolution of ^{18}F -Fluoride PET/CT compared to bone scintigraphy +/- SPECT or CT allows better diagnostic accuracy in detecting skeletal metastases in prostate, breast, lung and other cancers (30,31). As with bone scintigraphy, uptake of ^{18}F -Fluoride is not specific to metastases and benign bone lesions can cause false positives. However, specificity is improved by the ability to compare morphological characteristic on the CT component. In a National Oncology PET Registry (NOPR) trial of 3531 patients with prostate cancer, ^{18}F -Fluoride PET/CT changed

management from non-treatment to treatment in 47% at initial staging, 44% with suspected first bone metastasis and 52% of those with suspected progressive disease (32). Similar, significant changes in management were also seen in a further NOPR study of patients with breast, lung and other cancers (33).

The value of ^{18}F -Fluoride PET/CT in monitoring treatment response is less well described. However, early studies have shown potential for this application in patients treated with ^{223}Ra -chloride (34) and the ability to predict absorbed dose before therapy (35) and risk of bone marrow toxicity from this treatment (36). As both ^{18}F -Fluoride and ^{223}Ra -chloride share an osteoblastic mechanism of bone uptake, ^{18}F -Fluoride PET is well-suited as a theranostic agent in this setting.

A study of breast cancer patients treated with endocrine-based therapy showed that ^{18}F -Fluoride PET/CT showing an increase in SUV_{max} at 8 weeks could predict subsequent progressive disease with modest sensitivity (60%) but this could not be reliably differentiated from a flare in patients who ultimately responded (14). In another NOPR study evaluating ^{18}F -Fluoride PET/CT, a change in management in 40% of patients with prostate, breast or lung cancer was reported (37).

TUMOR-SPECIFIC IMAGING

^{18}F -Fluorodeoxyglucose PET/CT

There is evidence that different bone metastasis phenotypes exhibit different ^{18}F -FDG avidity. Osteoblastic metastases show lower uptake than osteolytic lesions, and the ^{18}F -FDG-avid osteolytic phenotype may be associated with a worse prognosis (38). This observation has been mostly reported in breast cancer where the low glycolytic activity in osteoblastic lesions occurs in both treated and untreated metastases, especially in lobular breast cancer metastases (39). In the majority of cancers, osteolytic metastases predominate, and several reports and meta-analyses confirm a greater sensitivity

and specificity for detecting bone metastases with ^{18}F -FDG PET/CT than with bone scintigraphy, particularly in breast cancer (38,40,41).

There is accumulating evidence that ^{18}F -FDG PET/CT may be helpful in monitoring systemic therapy (Fig. 3). There are several small retrospective series reporting that changes in SUV_{max} can monitor treatment response and predict time to SREs and to progression in breast cancer bone metastases (42-44). Two small prospective studies have confirmed the ability of ^{18}F -FDG PET/CT to predict time to SREs and / or time to progression, with superiority over ^{18}F -Fluoride which can be hampered by the flare phenomenon (14,45). In these studies, an increase in ^{18}F -Fluoride uptake caused by the flare phenomenon could not be reliably differentiated from progressive disease at early time points. In contrast, a metabolic flare is not commonly recognized with ^{18}F -FDG, although has been reported in a small cohort of patients with lung cancer treated with the antiangiogenic agent, bevacizumab when combined with chemotherapy (46). It is likely that some patients show heterogeneity of response between different metastases with ^{18}F -FDG and ^{18}F -Fluoride, an increasingly recognized phenomenon in cancer (14).

$^{18}\text{F}/^{11}\text{C}$ -Choline PET/CT

^{18}F -FDG demonstrates low uptake in hormone sensitive metastatic prostate cancer, although may show higher uptake in castrate-resistant prostate cancer where it has been used to monitor therapy response (47). For staging purposes there has been interest in using alternative tracers with higher uptake. Prostate cancer is associated with upregulation of choline transport and choline kinase expression with incorporation of choline into membranes of proliferating tumor cells. Both ^{11}C and ^{18}F labeling of choline has been described for staging high-risk prostate cancer at diagnosis and for evaluating biochemical recurrence (Fig. 2b). Active osteoblastic metastases show increased choline activity against the normal background bone marrow activity, and the rarer osteolytic phenotype shows

even higher uptake (48). For staging high-risk patients at diagnosis choline PET/CT has shown better diagnostic accuracy than bone scintigraphy (49,50) and also in patients with biochemical recurrence (51).

When ^{18}F -Choline has been compared to ^{18}F -Fluoride for detection of skeletal metastases from prostate cancer, some small bone marrow lesions were visible with ^{18}F -Choline but negative with ^{18}F -Fluoride (52). A further comparative cross sectional study of patients with bone metastases on hormone treatment showed that more sclerotic lesions with high Hounsfield Units on CT were more likely to be ^{18}F -Choline-negative but ^{18}F -Fluoride positive. This implies that lesions that have responded to treatment show choline metabolism that is switched off but that reparative osteoblastic activity, as shown by CT sclerosis and ^{18}F -Fluoride uptake, continues for longer (53). The data for the use of choline PET tracers for monitoring treatment response in bone metastases is conflicting. A study of 32 patients with castrate-resistant prostate cancer treated with docetaxel chemotherapy concluded that ^{11}C -Choline was of limited use for response assessment (54). A study evaluating response to the antiandrogen effects of enzalutamide with ^{18}F -Choline PET/CT suggested no additional benefit over PSA in predicting overall survival (55). However, a separate study of patients treated with the antiandrogen, abiraterone, reported that ^{18}F -Choline PET/CT predicted progression-free and overall survival (56).

^{18}F -Fluciclovine PET/CT

As an amino acid analog, ^{18}F -Fluciclovine shows some background normal bone marrow activity. Nevertheless, preclinical data showing ability to detect bone metastases (20) has been supported by subsequent clinical data with superiority over bone scintigraphy (Fig. 4) (21). To date, the role for this agent in monitoring treatment response in bone metastases is unknown.

⁶⁸Ga-PSMA PET/CT

PSMA tracers show minimal bone marrow activity and so PSMA expressing bone metastases show higher conspicuity compared to ¹⁸F-Choline (Fig. 5) (22). Several studies have reported higher sensitivity than bone scintigraphy (57-59) and similar or better sensitivity than ¹⁸F-Fluoride PET/CT (57,60). These results suggest that if PSMA PET/CT imaging is performed, then additional bone-specific imaging is not required in the majority of patients (58-60). However, one study showed a lower sensitivity for detecting bone metastases in patients with advanced disease scheduled for radionuclide therapy (61). These patients had all received previous conventional treatments and it is possible that a heterogeneous response, as has been described (62), had rendered tumor cells in some metastases metabolically quiescent (PSMA-negative) but with continued reparative osteoblastic activity (¹⁸F-Fluoride-positive), as has been suggested in a comparison between ¹⁸F-Choline and ¹⁸F-Fluoride (53).

False positives are rare but ⁶⁸Ga-PSMA uptake has been reported in Paget's disease (63). Although data for the use of PSMA PET for monitoring response in bone metastases is scarce, a metabolic flare to androgen deprivation therapy has been reported as a note of caution (64).

Whole-body MRI and Diffusion-Weighted Imaging

Whole-body MRI acquisitions are now feasible in less than 1 hour and with no ionizing radiation, high spatial and contrast resolution and new functional sequences, this modality is being adopted clinically for imaging the skeleton for metastatic disease (65,66). Several studies report high diagnostic accuracy in breast and prostate cancer, with similar accuracy to ¹⁸F-Fluoride, ¹⁸F-FDG and ¹¹C-Choline PET/CT (67-70).

There is increasing interest in using DW-MRI in conjunction with morphological sequences in WB-MRI to provide a quantitative measure of treatment response in skeletal metastases. Successful therapy leads to breakdown of tumor cells with loss of membrane integrity and cellularity and a

consequent increase in water diffusion in the extracellular space as measured by an increase in the ADC (5). Early reports confirm that an increase in ADC may predict clinical treatment response in prostate (71) and breast cancer (14).

A challenge with sclerotic bone lesions is that there are fewer protons to produce a signal, thus giving a low signal on T1 and T2-weighted images and a lower diffusion and ADC. There is a limitation in differentiating sclerosis following successful treatment from progressive disease although this has not been shown to have a significant negative diagnostic effect in prostate cancer (72).

PET/MRI

The MRI sequences performed as part of a whole-body MRI scan as discussed above can be replicated in PET/MRI acquisitions. Early data suggest there are synergistic advantages of combined PET/MRI imaging of the skeleton with ^{18}F -FDG (73) with an increase in anatomical delineation and diagnostic certainty in the evaluation of malignant bone lesions. Some inaccuracy in quantification of SUVs in skeletal lesions was also reported but this is likely to become less significant with the development of new attenuation correction algorithms from MRI data. A potential weakness of PET/MRI compared to PET/CT is that the CT component can give valuable additional information on bone lesion phenotype that MRI may be less able to determine.

CONCLUSION

Molecular and hybrid imaging of skeletal metastases can be divided into bone-specific and tumor-specific methods that have certain advantages and disadvantages depending on tumor phenotype and whether used for staging or response assessment. Improvements in scanning methodology with the advent of hybrid and new functional imaging, including SPECT/CT, PET/CT and WB-MRI with DW-MRI, allow better sensitivity and specificity in detecting bone metastases than was

previously possible. Early response assessment and prediction is improved with tumor-specific methods but the optimal method in each cancer type and after different types of treatment requires further research before firm recommendations can be given.

REFERENCES

1. D'Oronzo S, Coleman R, Brown J, Silvestris F. Metastatic bone disease: Pathogenesis and therapeutic options: Up-date on bone metastasis management. *J Bone Oncol.* 2018;15:004.
2. Franklin JM, Sharma RA, Harris AL, Gleeson FV. Imaging oligometastatic cancer before local treatment. *Lancet Oncol.* 2016;17:e406-414.
3. Mouridsen H, Gershanovich M, Sun Y, et al. Phase III study of letrozole versus tamoxifen as first-line therapy of advanced breast cancer in postmenopausal women: analysis of survival and update of efficacy from the International Letrozole Breast Cancer Group. *J Clin Oncol.* 2003;21:2101-2109.
4. Hoefeler H, Duran I, Hechmati G, et al. Health resource utilization associated with skeletal-related events in patients with bone metastases: results from a multinational retrospective—prospective observational study—a cohort from 4 European countries. *J Bone Oncol.* 2014;3:40-48.
5. Lecouvet FE, Talbot JN, Messiou C, Bourguet P, Liu Y, de Souza NM. EORTC Imaging Group. Monitoring the response of bone metastases to treatment with magnetic resonance imaging and nuclear medicine techniques: a review and position statement by the European Organisation for Research and Treatment of Cancer imaging group. *Eur J Cancer.* 2014;50:2519-2531
6. Cook GJR, Goh V. Functional and hybrid imaging of bone metastases. *J Bone Mineral Res.* 2018;33:961-972.
7. Eisenhauer EA, Therasse P, Bogaerts J, et al. New response evaluation criteria in solid tumours: revised RECIST guideline (version 1.1). *Eur J Cancer.* 2009;45:228e47.
8. Hamaoka T, Costelloe CM, Madewell JE, et al. Tumour response interpretation with new tumour response criteria vs the World Health Organisation criteria in patients with bone-only metastatic breast cancer. *Br J Cancer.* 2010;16;102:651-657.

9. Scher HI, Morris MJ, Stadler WM, et al; Prostate Cancer Clinical Trials Working Group 3. Trial design and objectives for castration-resistant prostate cancer: updated recommendations from the Prostate Cancer Clinical Trials Working Group 3. *J Clin Oncol*. 2016;34:1402-1418.
10. Paget S. The distribution of secondary growth in cancer of the breast. *Lancet*. 1889;1:571-573.
11. Guise TA, Mohammad KS, Clines G, et al. Basic mechanisms responsible for osteolytic and osteoblastic bone metastases. *Clin Cancer Res*. 2006;12:6213s-6216s.
12. Messiou C, Cook G, Reid AH, et al. The CT flare response of metastatic bone disease in prostate cancer. *Acta Radiol*. 2011;52:557-561.
13. Coleman RE, Mashiter G, Whitaker KB, Moss DW, Rubens RD, Fogelman I. Bone scan flare predicts successful systemic therapy for bone metastases. *J Nucl Med*. 1988;29:1354-1359.
14. Azad GK, Taylor BP, Green A, et al. Prediction of therapy response in bone-predominant metastatic breast cancer: comparison of [(18)F] fluorodeoxyglucose and [(18)F]-fluoride PET/CT with whole-body MRI with diffusion-weighted imaging. *Eur J Nucl Med Mol Imaging*. 2019;46:821-830.
15. Blake GM, Park-Holohan SJ, Cook GJ, Fogelman I. Quantitative studies of bone with the use of 18F-fluoride and 99mTc-methylene diphosphonate. *Semin Nucl Med*. 2001;31:28-49.
16. Cook GJ, Azad G, Padhani AR. Bone imaging in prostate cancer: the evolving roles of nuclear medicine and radiology. *Clin Transl Imaging*. 2016;4:439-447.
17. Anumula S, Wehrli SL, Magland J, Wright AC, Wehrli FW. Ultra-short echo-time MRI detects changes in bone mineralization and watercontent in OVX rat bone in response to alendronate treatment. *Bone*. 2010;46:1391-1399.
18. Cook GJ, Azad GK, Goh V. Imaging Bone Metastases in Breast Cancer: Staging and response assessment. *J Nucl Med*. 2016;57 Suppl 1:27S-33S.
19. Warburg O, Wind F, Negelein E. The metabolism of tumours in the body. *J Gen Physiol*. 1927;8:519-530

20. Oka S, Kanagawa M, Doi Y, Schuster DM, Goodman MM, Yoshimura H. PET Tracer (18)F-Fluciclovine can detect histologically proven bone metastatic lesions: A preclinical study in rat osteolytic and osteoblastic bone metastasis models. *Theranostics*. 2017;7:2048-2064.
21. Chen B, Wei P, Macapinlac HA, Lu Y. Comparison of 18F-Fluciclovine PET/CT and 99mTc-MDP bone scan in detection of bone metastasis in prostate cancer. *Nucl Med Commun*. 2019;40:940-946.
22. Afshar-Oromieh A, Zechmann CM, et al. Comparison of PET imaging with a (68)Ga-labelled PSMA ligand and (18)F-choline-based PET/CT for the diagnosis of recurrent prostate cancer. *Eur J Nucl Med Mol Imaging*. 2014;41:11-20.
23. Subramanian G, McAfee JG, Blair RJ, Kallfelz FA, Thomas FD. Technetium-99m-methylene diphosphonate--a superior agent for skeletal imaging: comparison with other technetium complexes. *J Nucl Med*. 1975;16:744-755.
24. Utsunomiya D, Shiraishi S, Imuta M, et al. Added value of SPECT/CT fusion in assessing suspected bone metastasis: comparison with scintigraphy alone and nonfused scintigraphy and CT. *Radiology*. 2006;238:264-271.
25. Helyar V, Mohan HK, Barwick T, et al. The added value of multislice SPECT/CT in patients with equivocal bony metastasis from carcinoma of the prostate. *Eur J Nucl Med Mol Imaging*. 2010;37:706-713.
26. Coombes RC, Dady P, Parsons C, et al. Assessment of response of bone metastases to systemic treatment in patients with breast cancer. *Cancer*. 1983;52:610-614.
27. Doot RK, Muzi M, Peterson LM, et al. Kinetic Analysis of 18F-Fluoride PET Images of Breast Cancer Bone Metastases. *J Nucl Med*. 2010;51:521-527.
28. Yu EY, Duan F, Muzi M, et al. Castration-resistant prostate cancer bone metastasis response measured by 18F-fluoride PET after treatment with dasatinib and correlation with progression-free

survival: results from American College of Radiology Imaging Network 6687. *J Nucl Med.* 2015;56:354-360.

29. Azad GK, Siddique M, Taylor B, et al. Is response assessment of breast cancer bone metastases better with measurement of (18)F-Fluoride metabolic flux than with measurement of (18)F-Fluoride PET/CT SUV? *J Nucl Med.* 2019;60:322-327.

30. Even-Sapir E, Metser U, Flusser G, et al. Assessment of malignant skeletal disease: initial experience with 18F-Fluoride PET/CT and comparison between 18F-Fluoride PET and 18F-Fluoride PET/CT. *J Nucl Med.* 2004;45:272-278.

31. Damle N, Bal C, Bandopadhyaya GP, et al. The role of 18F-fluoride PET-CT in the detection of bone metastases in patients with breast, lung and prostate carcinoma: a comparison with FDG PET/CT and 99mTc-MDP bone scan. *Jpn J Radiol.* 2013;31:262-269.

32. Hillner BE, Siegel BA, Hanna L, Duan F, Shields AF, Coleman RE. Impact of 18F-fluoride PET in patients with known prostate cancer: initial results from the National Oncologic PET Registry. *J Nucl Med.* 2014;55:574-581.

33. Hillner BE, Siegel BA, Hanna L, et al. Impact of (18)F-Fluoride PET on intended management of patients with cancers other than prostate cancer: results from the National Oncologic PET Registry. *J Nucl Med.* 2014;55:1054-1061.

34. Cook GJR, Parker C, Chua S, Johnson B, Aksnes AK, Lewington VJ. 18F-fluoride PET: changes in uptake as a method to assess response in bone metastases from castrate-resistant prostate cancer patients treated with 223Ra-chloride (Alpharadin). *Eur J Nucl Med Mol Imaging Res.* 2011;1:4.

35. Murray I, Chittenden SJ, Denis-Bacelar AM, et al. The potential of 223Ra and 18F-fluoride imaging to predict bone lesion response to treatment with 223Ra-dichloride in castration-resistant prostate cancer. *Eur J Nucl Med Mol Imaging.* 2017;44:1832-1844.

36. Etchebehere EC, Araujo JC, Milton DR, et al. Skeletal tumor burden on baseline 18F-Fluoride PET/CT predicts bone marrow failure after 223Ra therapy. *Clin Nucl Med*. 2016;41:268-273.
37. Hillner BE, Siegel BA, Hanna L, Duan F, Quinn B, Shields AF. 18F-fluoride PET used for treatment monitoring of systemic cancer therapy: results from the National Oncologic PET Registry. *J Nucl Med*. 2015;56:222-228.
38. Cook GJ, Houston S, Rubens R, Maisey MN, Fogelman I. Detection of bone metastases in breast cancer by 18FDG PET: differing metabolic activity in osteoblastic and osteolytic lesions. *J Clin Oncol*. 1998;16:3375-3379.
39. Dashevsky BZ, Goldman DA, Parsons M, et al. Appearance of untreated bone metastases from breast cancer on FDG PET/CT: importance of histologic subtype. *Eur J Nucl Med Mol Imaging*. 2015;42:1666-1673.
40. Shie P, Cardarelli R, Brandon D, Erdman W, Abdulrahim N. Meta-analysis: comparison of F-18 Fluorodeoxyglucose-positron emission tomography and bone scintigraphy in the detection of bone metastases in patients with breast cancer. *Clin Nucl Med*. 2008;33:97-101.
41. Rong J, Wang S, Ding Q, Yun M, Zheng Z, Ye S. Comparison of 18FDG PET-CT and bone scintigraphy for detection of bone metastases in breast cancer patients. A meta-analysis. *Surg Oncol*. 2013;22:86-91.
42. Stafford SE, Gralow JR, Schubert EK, et al. Use of serial FDG PET to measure the response of bone-dominant breast cancer to therapy. *Acad Radiol*. 2002;9:913–921.
43. Tateishi U, Gamez C, Dawood S, Yeung HW, Cristofanilli M, Macapinlac HA. Bone metastases in patients with metastatic breast cancer: morphologic and metabolic monitoring of response to systemic therapy with integrated PET/CT. *Radiology*. 2008;247:189–196.
44. Specht JM, Tam SL, Kurland BF, et al. Serial 2-[18F] fluoro-2-deoxy-D-glucose positron emission tomography (FDG-PET) to monitor treatment of bone-dominant metastatic breast cancer predicts time to progression (TTP). *Breast Cancer Res Treat*. 2007;105:87–94.

45. Peterson LM, O'Sullivan J, Wu QV, et al. Prospective study of serial (18)F-FDG PET and (18)F-Fluoride PET to predict time to skeletal-related events, time to progression, and survival in patients with bone-dominant metastatic breast cancer. *J Nucl Med*. 2018;59:1823-1830.
46. Krupitskaya Y, Eslamy HK, Nguyen DD, Kumar A, Wakelee HA. Osteoblastic bone flare on F18-FDG PET in non-small cell lung cancer (NSCLC) patients receiving bevacizumab in addition to standard chemotherapy. *J Thorac Oncol*. 2009;4:429-431.
47. Morris MJ, Akhurst T, Larson SM, et al. Fluorodeoxyglucose positron emission tomography as an outcome measure for castrate metastatic prostate cancer treated with antimicrotubule chemotherapy. *Clin Cancer Res*. 2005;11:3210–3216.
48. Ceci F, Castellucci P, Graziani T, et al. 11C-choline PET/CT identifies osteoblastic and osteolytic lesions in patients with metastatic prostate cancer. *Clin Nucl Med*. 2015;40:e265–e270.
49. Evangelista L, Cimitan M, Zattoni F, Guttilla A, Zattoni F, Saladini G. Comparison between conventional imaging (abdominal-pelvic computed tomography and bone scan) and [(18)F]choline positron emission tomography/computed tomography imaging for the initial staging of patients with intermediate-to high-risk prostate cancer: a retrospective analysis. *Scand J Urol*. 2015;49:345–353.
50. Wondergem M, van der Zant FM, van der Ploeg T, Knol RJ. A literature review of 18F-fluoride PET/CT and 18Fcholine or 11C-choline PET/CT for detection of bone metastases in patients with prostate cancer. *Nucl Med Commun*. 2013;34:935–945.
51. Picchio M, Spinapolice EG, Fallanca F, et al. [11C]Choline PET/CT detection of bone metastases in patients with PSA progression after primary treatment for prostate cancer: comparison with bone scintigraphy. *Eur J Nucl Med Mol Imaging*. 2012;39:13–26.
52. Beheshti M, Vali R, Waldenberger P, et al. Detection of bone metastases in patients with prostate cancer by 18F fluorocholine and 18F fluoride PET-CT: a comparative study. *Eur J Nucl Med Mol Imaging*. 2008;35:1766–1774.

53. Beheshti M, Vali R, Waldenberger P, et al. The use of F-18 choline PET in the assessment of bone metastases in prostate cancer: correlation with morphological changes on CT. *Mol Imaging Biol.* 2010;12:98-107.
54. Schwarzenböck SM, Eiber M, Kundt G, et al. Prospective evaluation of [(11)C]Choline PET/CT in therapy response assessment of standardized docetaxel first-line chemotherapy in patients with advanced castration refractory prostate cancer. *Eur J Nucl Med Mol Imaging.* 2016;43:2105-2113.
55. De Giorgi U, Caroli P, Scarpi E, et al. (18)F-Fluorocholine PET/CT for early response assessment in patients with metastatic castration-resistant prostate cancer treated with enzalutamide. *Eur J Nucl Med Mol Imaging.* 2015;42:1276–1283.
56. De Giorgi U, Caroli P, Burgio SL, et al. Early outcome prediction on 18F-fluorocholine PET/CT in metastatic castration resistant prostate cancer patients treated with abiraterone. *Oncotarget.* 2014;5:12448–12458.
57. Zhou J, Gou Z, Wu R, Yuan Y, Yu G, Zhao Y. Comparison of PSMA-PET/CT, choline-PET/CT, NaF-PET/CT, MRI, and bone scintigraphy in the diagnosis of bone metastases in patients with prostate cancer: a systematic review and meta-analysis. *Skeletal Radiol.* 2019;48:1915-1924.
58. Lengana T, Lawal IO, Boshomane TG, et al. (68)Ga-PSMA PET/CT replacing bone scan in the initial staging of skeletal metastasis in prostate cancer: A fait accompli? *Clin Genitourin Cancer.* 2018;16:392-401.
59. Pyka T, Okamoto S, Dahlbender M, et al. Comparison of bone scintigraphy and (68)Ga-PSMA PET for skeletal staging in prostate cancer. *Eur J Nucl Med Mol Imaging.* 2016;43:2114-2121.
60. Rowe SP, Li X, Trock BJ, et al. Prospective Comparison of PET Imaging with PSMA-targeted (18)F-DCFPyL versus Na(18)F for Bone Lesion Detection in Patients with Metastatic Prostate Cancer. *J Nucl Med.* 2020;61:183-188.

61. Uprimny C, Sviriydenka A, Fritz J, et al. Comparison of [(68)Ga]Ga-PSMA-11 PET/CT with [(18)F]NaF PET/CT in the evaluation of bone metastases in metastatic prostate cancer patients prior to radionuclide therapy. *Eur J Nucl Med Mol Imaging*. 2018;45:1873-1883.
62. Morin F, Beauregard JM, Bergeron M, et al. Metabolic imaging of prostate cancer reveals inpatient intermetastasis response heterogeneity to systemic therapy. *Eur Urol Focus*. 2017;3:639-642.
63. Artigas C, Alexiou J, Garcia C, et al. Paget bone disease demonstrated on (68)Ga-PSMA ligand PET/CT. *Eur J Nucl Med Mol Imaging*. 2016;43:195-196.
64. Zacho HD, Petersen LJ. Bone flare to androgen deprivation therapy in metastatic, hormone-sensitive prostate cancer on 68Ga-Prostate-Specific Membrane Antigen PET/CT. *Clin Nucl Med*. 2018;43:e404-e406.
65. Lecouvet FE. Whole-Body MR Imaging: Musculoskeletal applications. *Radiology*. 2016;279:345-365.
66. Wu LM, Gu HY, Zheng J, et al. Diagnostic value of whole-body magnetic resonance imaging for bone metastases: a systematic review and meta-analysis. *J Magn Reson Imaging*. 2011;34:128-135.
67. Mosavi F, Johansson S, Sandberg DT, Turesson I, Sörensen J, Ahlström H. Whole-body diffusion-weighted MRI compared with (18)F-NaF PET/CT for detection of bone metastases in patients with high-risk prostate carcinoma. *AJR Am J Roentgenol*. 2012;199:1114–1120.
68. Jambor I, Kuisma A, Ramadan S, et al. Prospective evaluation of planar bone scintigraphy, SPECT, SPECT/CT, 18F-NaF PET/CT and whole body 1.5T MRI, including DWI, for the detection of bone metastases in high risk breast and prostate cancer patients: SKELETA clinical trial. *Acta Oncol*. 2016;55:59-67.
69. Luboldt W, Küfer R, Blumstein N, et al. Prostate carcinoma: diffusion-weighted imaging as potential alternative to conventional MR and 11C-choline PET/CT for detection of bone metastases. *Radiology*. 2008;249:1017–1025.

70. Heusner TA, Kuemmel S, Koeninger A, et al. Diagnostic value of diffusion-weighted magnetic resonance imaging (DWI) compared to FDG PET/CT for whole-body breast cancer staging. *Eur J Nucl Med Mol Imaging*. 2010;37:1077–1086.
71. Perez-Lopez R, Mateo J, Mossop H, et al. Diffusion-weighted imaging as a treatment response biomarker for evaluating bone metastases in prostate cancer: A pilot study. *Radiology*. 2017;283:168-177.
72. Messiou C, Collins DJ, Morgan VA, Bianchini D, de Bono JS, de Souza NM. Use of apparent diffusion coefficient as a response biomarker in bone: effect of developing sclerosis on quantified values. *Skeletal Radiol*. 2014;43:205-208.
73. Eiber M, Takei T, Souvatzoglou M, Mayerhoefer ME, et al. Performance of whole-body integrated 18F-FDG PET/MR in comparison to PET/CT for evaluation of malignant bone lesions. *J Nucl Med*. 2014;55:191-197.

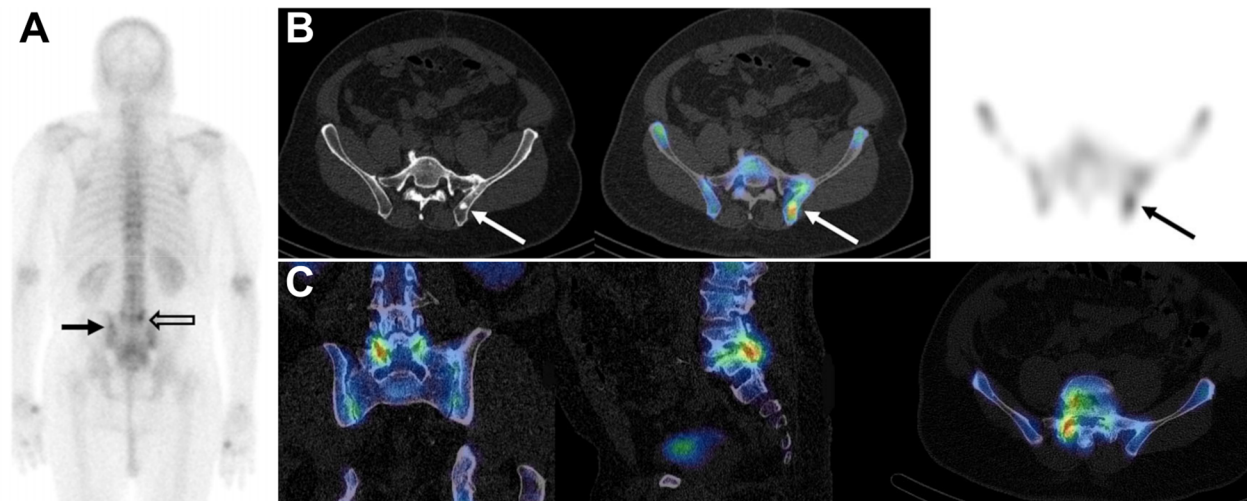


Figure 1. A patient with high-risk newly diagnosed prostate cancer. a) ^{99m}Tc -MDP posterior planar bone scan, b) from left to right: CT, fused and SPECT transaxial images through the iliac bones and c) coronal, sagittal and transaxial fused SPECT/CT images of the lower lumbar spine. A metastasis showing CT sclerosis and ^{99m}Tc -MDP uptake is faintly visible on the planar image (black arrow) but more clearly shown on the SPECT/CT images (arrows). In contrast, abnormal activity in the lower lumbar spine on the planar image (open arrow) can be seen to relate to benign facet joint changes on the SPECT/CT images.

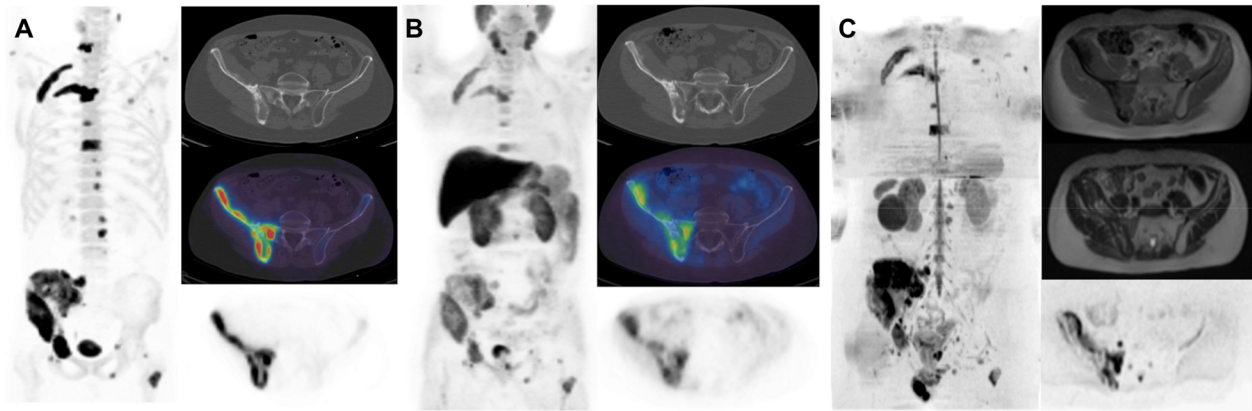


Figure 2. A patient with metastatic prostate cancer. a) ^{18}F -Fluoride and b) ^{11}C -Choline: Maximum intensity projection (left), transaxial pelvis CT (upper), fused PET/CT (middle) and PET (lower). c) MRI Maximum intensity projection image (high b value - $b800\text{ s/mm}^2$) (left), transaxial pelvis T1-weighted Dixon (upper), T2-weighted (middle) and b800 diffusion-weighted (lower) images. Corresponding increased ^{18}F -Fluoride and ^{11}C -Choline uptake is present in several bone metastases corresponding to low signal on T1, mixed signal on T2 and high signal on the b800 images.

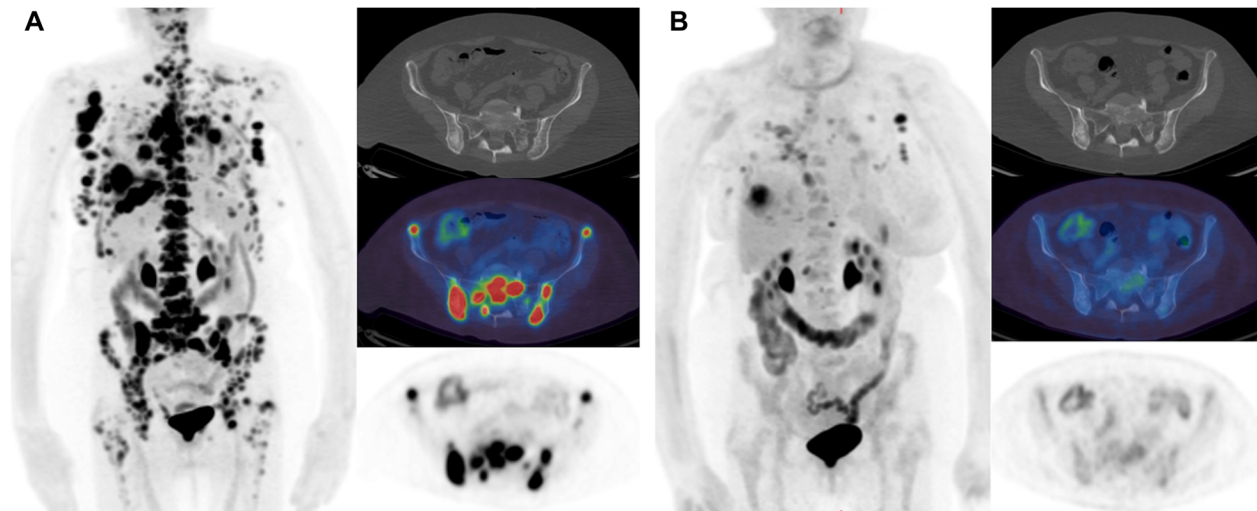


Figure 3. A patient with metastatic breast cancer. ^{18}F -FDG PET/CT scans a) before and b) 8 weeks after commencing endocrine therapy. Maximum intensity projection (left), transaxial pelvis CT (upper), fused PET/CT (middle) and PET (lower). Extensive bone and soft tissue metastases show a significant reduction in uptake at most sites in keeping with a treatment response. Note the iliac bones appear slightly more sclerotic on the CT component.

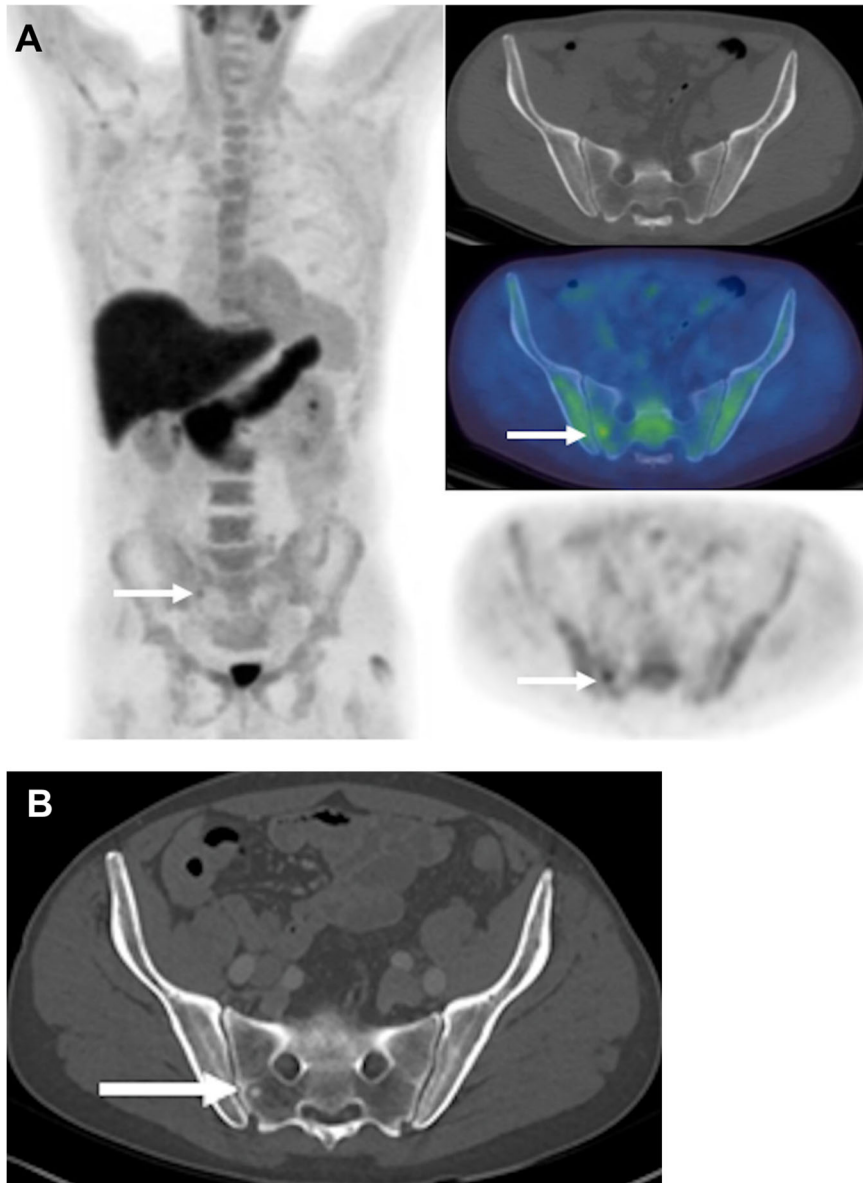


Figure 4. A patient with biochemical recurrence (PSA 0.52 ng/mL) 11 months after prostatectomy for Gleason 4+5 prostate cancer. a) ^{18}F -Fluciclovine PET/CT maximum intensity projection (left), transaxial pelvis CT (upper), fused PET/CT (middle) and PET (lower). A subtle focus of increased uptake is present in the right side of the sacrum (arrows) but is occult on the CT component. The patient was started on hormone therapy and subsequently the lesion became sclerotic in response to therapy (b) (arrow). (Courtesy of Blue Earth Diagnostics Ltd).

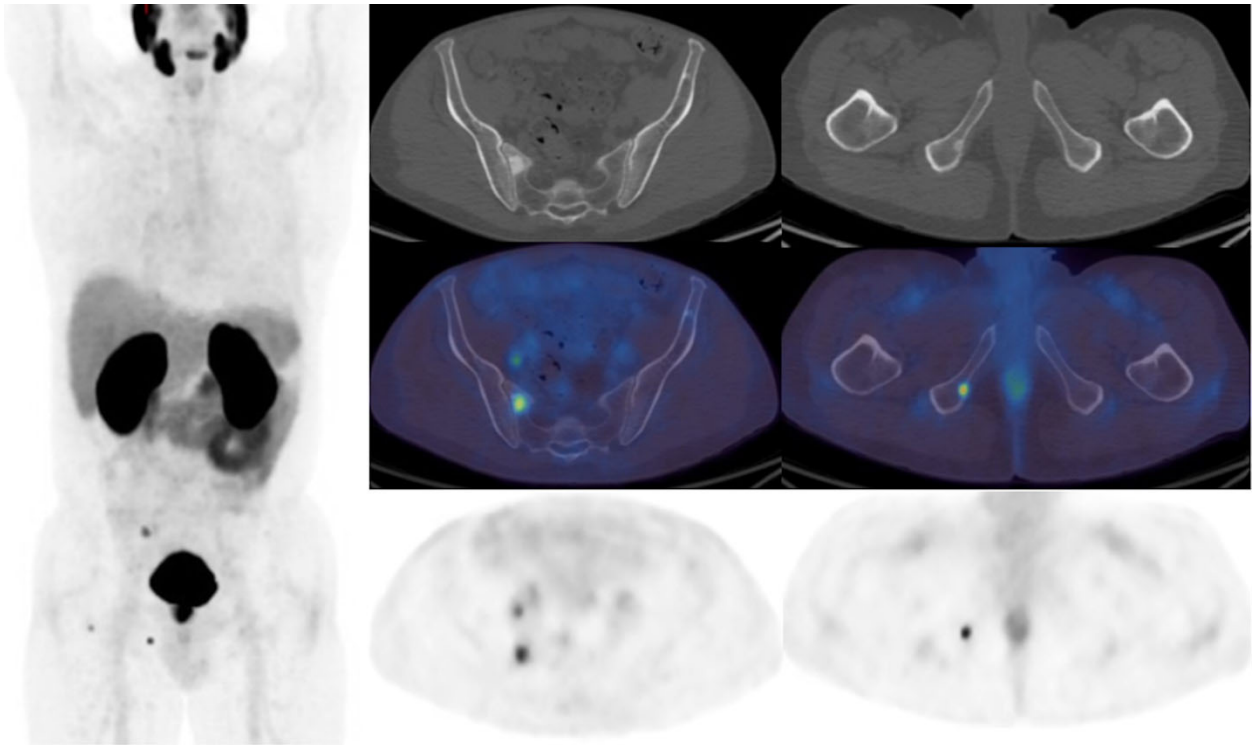


Figure 5. A patient with a new diagnosis of Gleason 4+5 prostate cancer (PSA 20.8 ng/mL). ^{68}Ga -PSMA PET/CT. Maximum intensity projection (left), transaxial pelvis CT (upper row), fused PET/CT (middle row) and PET (lower row). As well as increased uptake in the prostate gland visible in the maximum intensity projection image, there are focal areas of increased tracer corresponding to sclerotic lesions in the right sacrum and right ischium. A further bone lesion is present in the right hip on the maximum intensity projection image and uptake in a right pelvic node is also visible on the upper transaxial PET images.

TABLES

Radiopharmaceutical	Mechanism	Usual injected activity*	Scan time post-injection	Clinical utility	References
^{99m} Tc-MDP	Bone	600-1110 MBq	2-5 h	Staging, restaging, response assessment	5,6,8,9,16,18,23,24, 25,26
¹⁸ F-Fluoride	Bone	185-370 MBq	30-120 min	Staging, response assessment, prognosis	6,14,16,18,27,28,29,30,31, 32,33,34,35,37,45,50
¹⁸ F-FDG	Tumor	370-740 MBq	45-90 min	Staging, restaging, response assessment, prognosis	5,6,14,18,31,38,39,40,41, 42,43,44,45,47
¹¹ C-Choline	Tumor	370-740 MBq	2-5 min	Staging, restaging, response assessment	48,50,51,54,69
¹⁸ F-Choline	Tumor	370 MBq	60 min	Staging, restaging, response assessment	49,50,52,53,55,56
¹⁸ F-Fluciclovine	Tumor	370 MBq	3-5 min	Restaging	21
⁶⁸ Ga-PSMA	Tumor	100-200 MBq	50-100 min	Staging, restaging	22,57,58,59

Table 1. Radiopharmaceuticals and their clinical utility in imaging bone metastases

MDP: methylene diphosphonate, FDG: Fluorodeoxyglucose, PSMA: prostate-specific membrane antigen